Measuring the Sea Breeze from QuikSCAT Scatterometry

Sarah T. Gille

Scripps Institution of Oceanography and Department of Mechanical and Aerospace Engineering, University of California, San Diego

Stefan G. Llewellyn Smith

Department of Mechanical and Aerospace Engineering, University of California, San Diego

Shira M. Lee

Massachusetts Institute of Technology

Abstract. Differences between morning and evening winds from QuikSCAT scatterometer measurements are analyzed to diagnose the diurnal variability of the wind over the ocean. A statistically significant signal, associated with the sea breeze, is present along most of the world's coastlines. Significant diurnal variability is also present mid-ocean in the easterly trade wind belts.

1. Introduction

Sea breezes are caused by differential heating of the land and ocean. As the land warms during the day, denser air from the adjacent ocean flows over the land. At night, the flow pattern reverses. *Simpson* [1994] provides a comprehensive overview of the sea breeze, which has implications for coastal physical oceanography, coastal meteorology, and atmospheric pollution.

The structure of the sea breeze over land has been observed for more than a century using land-based meteorological stations [e.g. *Davis et al.*, 1890]. In past studies aircraft measurements, regional radar, and meteorological buoys have been used to probe the offshore structure of the sea breeze [e.g. *Atkins et al.*, 1995]. These studies have elucidated the characteristics of the sea breeze only in areas where field observations have been conducted. For example, along the Baltic coast the landward and seaward reach of the sea breeze are about the same, with effects felt approximately 50 km inland and out to sea [*Rossi*, 1957; *Simpson*, 1994]. Similar estimates on a global scale have not been possible to date.

Satellite scatterometry now allows us to obtain measurements of wind speed and direction globally, including along ice-free coastlines. This study uses vector wind fields obtained from the QuikSCAT satellite scatterometer to examine the amplitude, direction, and offshore extent of the sea breeze.

2. Scatterometer Data

The QuikSCAT satellite was launched in July 1999. Its SeaWinds scatterometer measures backscattered microwave power, which is translated into 10-m wind speed and direction along an 1800 km wide swath. The satellite orbit is optimized to measure winds over 90% of the Earth at least once per day. QuikSCAT

Paper number .
0094-8276/02/$5.00

follows a sun-synchronous orbit: the nadir beam, directly below the satellite, measures winds around 6:00 local time for ascending satellite passes and around 18:00 local time for descending satellite passes [*Longu*, 2001]. Figure 1 shows the time range of measurements as a function of latitude. Compared to the 3- to 6-hourly Comprehensive Ocean-Atmosphere Data Set used by *Dai and Deser* [1999] to study diurnal variations in global surface winds, QuikSCAT offers coarser temporal sampling but higher spatial resolution. The major focus of this paper is the coastal sea breeze, which requires high spatial resolution sampling.

Gridded products have been developed based on QuikSCAT winds. However, we work with swath winds to retain the original spatial resolution and temporal sampling information in the data. The winds are initially processed by Remote Sensing Systems (www.remss.com). We use compact level 2B data files produced by Florida State University's Center for Ocean-Atmosphere Prediction Studies. The data in this analysis span a 3 year period from 31 July 1999 to 30 July 2002. Swath winds are reported in 25 km by 25 km pixels. The pixels have different coordinates each day, depending on the exact location of the satellite. For this analysis, we averaged eastward (u) and northward (v) components of the morning and evening data into 0.4° latitude by 0.4° longitude bins for the global ocean. Results based on 0.2° boxes are consistent with the results reported here.

3. Analysis of the Sea Breeze

Figure 2a shows for the global ocean the amplitude and direction of the mean wind $\bar{\mathbf{u}} = \frac{1}{2}(\mathbf{u}_{am} + \mathbf{u}_{pm})$, representing the average of morning and evening passes, where $\mathbf{u} \equiv (u, v)$ is the vector wind. For each box the error of the wind components u and v was estimated for both morning and evening winds by computing twice the standard deviation of u and v divided by the square root of the number of samples. The error of the mean is then half the square root of the sum of these four error components squared. White regions in Figure 2a indicate places where the mean wind is not statistically different from zero.

Because the sea breeze is characterized by a reversal of the wind on a daily basis, we computed the difference between the morning and evening satellite passes to identify the sea breeze. Figure 2b shows the amplitude and direction of the difference $\Delta\mathbf{u} \equiv \mathbf{u}_{am} - \mathbf{u}_{pm}$. The error in $\Delta\mathbf{u}$ is twice the error in $\bar{\mathbf{u}}$. Speeds and directions have been plotted only if the difference between morning and evening passes is statistically different from zero.

Statistically significant values of $\Delta\mathbf{u}$ occur along most of the coastlines of the world. However, the most visible feature in Figure 2b is the large band of small but statistically significant $\Delta\mathbf{u}$ in the trade wind belt, between 30°S and 30°N. The open-ocean vectors in Figure 2b indicate that flow is more poleward in the morning and more equatorward in the evening, implying a divergence of the wind in the morning and a convergence in the evening, most likely linked to enhanced daytime rising air motions in the tropics relative to the subtropics. This is consistent with *Dai and Deser* [1999], who reported a maximum in surface wind divergence around 6:00 in much of the tropical Pacific. The zonal bands of white in between about 5°N and 10°N in Figure 2b appear to coincide with the Intertropical Convergence Zone.

The easterly trade winds in Figure 2a average between 5 and 10 m s^{-1}, so the diurnal cycle in Figure 2b represents a small perturbation to this mean flow. For comparison, in Figure 2c, the amplitude and direction of $\Delta\mathbf{u}$ is plotted only in locations where it exceeds the component of mean flow in the same direction, i.e. $|\Delta\mathbf{u}|^2 > |\Delta\mathbf{u} \cdot \bar{\mathbf{u}}|$, so that the wind reverses direction between

morning and evening. This flow reversal occurs primarily along coastlines, with directional vectors in Figure 2c indicating that the winds are offshore in the morning and onshore in the evening. This reversal can be thought of as a signature of the sea breeze. Significant sea breezes are found along most of the coastlines of the world, including for example, along the western Mediterranean Sea, along the west coast of Africa, and around most of the islands of the Indonesian Archipelago. The sea breeze speeds plotted in Figure 2c are strongest at points closest to the coast and decrease with distance offshore. However, along the west coast of South America and the southwest coast of Africa, the sea breeze appears displaced from the coast. Poleward of 50°, the sea breeze is noticeably diminished, and in many places no diurnal difference is observed. The lack of sea breeze signal at high latitudes is not an artifact of the temporal sampling: narrowing the morning and evening time window to 3 hours in order to ensure that high-latitude measurements were from the same time of day had little impact on the results.

The sea breeze is generated by solar heating of the land, and the corresponding sea-breeze front propagates onshore as a gravity current. Because of the twice-daily sampling provided by QuikSCAT, we cannot see this propagation. In an analysis of buoy data off the coast of southern California, *Lerczak et al.* [2001] found that maximum onshore winds on the shoreline were 2.7 hours after local noon, while 220 km offshore, the maximum onshore winds occurred 9 hours after local noon. Since QuikSCAT measures six hours after local noon, we expect to sample the maximum amplitude of the diurnal cycle at a location several hundred kilometers offshore. If QuikSCAT observations were collected closer to noon, we might expect to see a more pronounced sea breeze in coastal bins, and the white areas off the west coasts of South America and Africa might not extend all the way to the coast.

Sea breezes are predicted to rotate anticyclonically through the course of the day [e.g. *Haurwitz*, 1947]. Depending on the timing of solar forcing effects compared with the QuikSCAT sampling time, the sea breeze could be observed with a variety of different orientations relative to the coastline. The temporal and spatial sampling of the scatterometer did not allow us to investigate the rotation in detail. *Lerczak et al.* [2001] showed that the major axis of wind variability on the beach in San Diego is offset between 30° and 45° from the axis of the coastline. In contrast, at locations between 60 and 220 km offshore, the major axis of wind variability was perpendicular to the coast. The results in Figure 2b,c are consistent with *Lerczak et al.*'s [2001] findings, showing that in the locations resolved by QuikSCAT, which are generally at least 30 km from the shore, the sea breeze is perpendicular to the coastline.

4. Offshore Extent of the Sea Breeze

The offshore extent of the sea breeze varies with location: it is about 200 km off the west coast of the Sahara Desert in Africa, 400 km south of Australia, and extends northward from the Yucatán Peninsula across almost the entire Gulf of Mexico. Using linear theory, *Niino* [1987] argued that the offshore extent of the sea breeze should vary by about a factor of 3 as a function of latitude, with the sea breeze extending further out to sea in lower latitudes, as is observed here. Numerical simulations have also found this trend [*Yan and Anthes*, 1987; *Ciesielski et al.*, 2001].

In most locations the sea breeze extends out to sea from the coast, but off the west coasts of South America and Africa, as noted above, it does not. Both locations are in the trade-wind belt and are distinguished by high mountains not far from the coastline. Adjacent to the Andes, in particular, mean winds (Figure 2a) and the daily cycle (Figure 2b) both flow parallel to the coast, probably as

a result of topographic constraints which inhibit flow perpendicular to the coast. Since the mean winds are much stronger than the morning-evening difference, no statistically significant flow reversal is possible. Further offshore the diurnal difference is orthogonal to the mean flow, resulting in the offshore displacement of the sea breeze shown here. Figure 2b also suggests that the trade wind cycle is amplified near these mountains; in both locations mean wind differences exceeding 1 m s^{-1} extend 750 km or more off shore. This is consistent with *Dai and Deser* [1999], who reported strong diurnal cycles over elevated topography, and with *Jury and Spencer-Smith* [1988], who noted that trade winds tend to accelerate at night downstream of topography.

Since the sea breeze depends on the diurnal heating of the land, we had expected that land surface type, which affects heat capacity and cloud cover over land, might also influence the offshore extent of the sea breeze. We therefore compared the sea breeze magnitude at each point within 1100 km of the coast with the land surface type for the nearest point on land [*Dickinson et al.*, 1986]. Although the offshore extent of sea breeze varies strongly with latitude, within 10° wide latitude bands, we saw no clear dependence on land surface type. For example, the sea breeze west of the Sahara Desert extends no further offshore than the sea breeze west of the more forested coast of Mexico at the same latitude.

5. Seasonal Effects

In mid-latitude observations, the sea breeze is commonly thought of as a summertime phenomenon. Therefore we repeated our analysis from Figure 2c for December–February, representing the Southern Hemisphere summer, and for June–August, representing the Northern Hemisphere summer. Figures 3a and b show the seasonal sea breeze signal along the South American coastlines, here for 0.2° by 0.2° boxes. In summer (DJF) a strong sea breeze effect exists along the east coast. In winter when the land-ocean temperature contrast is reduced, the sea breeze largely disappears. Similar effects occur along other coastlines at mid- to high-latitudes (not shown). Summer-only data do not indicate the presence of a significant sea breeze anywhere that does not also have a clear sea breeze signal in the annual data shown in Figures 2b,c. Within the easterly trade wind belt (e.g. the northern 15° of Figure 3a,b), the sea breeze does not show a strong seasonal cycle, presumably because seasonal temperature variations are small in the tropics.

6. Summary and Discussion

We have analyzed three years of QuikSCAT wind observations and have shown that statistically significant diurnal variability of the wind occurs along most coastlines equatorward of 50° latitude and in the easterly trade winds. Along most coasts, this diurnal variability results in an onshore-offshore reversal of flow that is characteristic of the sea breeze. Enhanced diurnal variability can extend 1000 km or more off shore downstream of major orographic features such as the Andes. However adjacent to coastal mountains, mean winds and their diurnal variations both tend to be aligned parallel to the coast; in such situations, if the diurnal variations are smaller in magnitude than the mean winds, then no flow reversal is observed, as is the case near the Andes in Figure 2c. Our results support the conjecture of *Simpson et al.* [2002] that the sea breeze forces diurnal variability in the coastal ocean 150 km offshore from Namibia.

Diurnal variations in wind are not well sampled by twice-daily observations. The situation should improve after the launch of the ADEOS-II satellite, which will provide scatterometer measure-

ments at 10:30 and 22:30.

Acknowledgments. This project originated out of discussions with J.H. Simpson. Discussions with C.E. Dorman, M.C. Hendershott and J.R. Norris helped with the analysis and presentation of these results. This work was supported by the NASA Ocean Vector Wind Science Team, JPL contract 1222984.

Figure 2 caption: Amplitude (color) and direction (vectors) of winds. (a) Average of mean morning and evening winds. (b) Mean morning minus evening winds. (c) As (b), but regions where the flow does not reverse are excluded. Wind velocity differences that are not statistically significant are shown as white. Vectors are plotted at 4 degree intervals, except in (a), where the zonal separation between vectors is 6 degrees. Landmasses are shaded to show elevation above sea level, based on the ETOPO2 data base.

References

Atkins, N. T., R. M. Wakimoto, and T. M. Weckwerth, Observations of the sea-breeze front during CaPE. Part II: Dual-Doppler and aircraft analysis, *Mon. Wea. Rev*, *123*, 944–969, 1995.

Ciesielski, P. E., W. H. Schubert, and R. H. Johnson, Diurnal variability of the marine boundary layer during ASTEX, *J. Atmos. Sci.*, *58*, 2355–2376, 2001.

Dai, A., and C. Deser, Diurnal and semidiurnal variations in global suface wind divergence fi elds, *J. Geophys. Res.*, *104*, 31,109–31,125, 1999.

Davis, W. M., L. G. Schultz, and R. de C. Ward, An investigation of the sea-breeze, *Ann. Astron. Observ. Harvard Coll.*, *21*, 215–265, 1890.

Dickinson, R. E., A. Henderson-Sellers, P. J. Kennedy, and M. F. Wilson, Biosphere-atmosphere transfer scheme (BATS) for the NCAR community climate model, *Tech. Rep. NCAR/TN275+STR*, NCAR, Boulder, CO, 1986, 69 pp.

Haurwitz, B., Comments on the sea-breeze circulation, *J. Meteorol.*, *4*, 1–8, 1947.

Jury, M., and G. Spencer-Smith, Doppler sounder observations of trade winds and sea breezes along the African West Coast near 34°S, 19°E, *Boundary-Layer Meteorol.*, *44*, 373–405, 1988.

Lerczak, J. A., M. C. Hendershott, and C. D. Winant, Observations and modeling of coastal internal waves driven by a diurnal sea breeze, *J. Geophys. Res.*, *106*, 19,715–19,729, 2001.

Longu, T., QuikSCAT science data product user's manual, overview and geophysical data products, *Tech. Rep. D-18053*, Jet Propulsion Laboratory, 2001.

Niino, H., The linear theory of land and sea breeze circulation, *J. Meteorol. Soc. Japan*, *65*, 901–921, 1987.

Rossi, V., Land- und Seewind an der fi nnischen Küsten, *Mitteilungen der Meteorologischen Zentralanstalt*, 1957.

Simpson, J. E., *Sea Breeze and Local Wind*, Cambridge University Press, Cambridge, England, 1994.

Simpson, J. H., P. Hyder, T. P. Rippeth, and I. M. Lucas, Forced oscillations near the critical latitude for diurnal-inertial resonance, *J. Phys. Oceanogr.*, *32*, 177–187, 2002.

Yan, H., and R. A. Anthes, The effect of latitude on the sea breeze, *Mon. Wea. Rev.*, *115*, 936–956, 1987.

Sarah T. Gille, Scripps Institution of Oceanography, University of California San Diego, La Jolla, CA 92093-0230 (sgille@ucsd.edu)

(Received _____.)

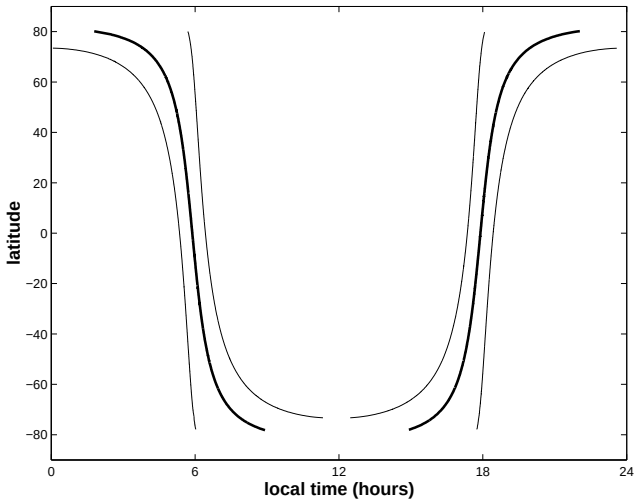

Figure 1. Time of day of ascending and descending QuikSCAT satellite passes. Thick lines indicate the time of day for the nadir beam, while thin lines indicate the time for the eastern and western edges of the swath.

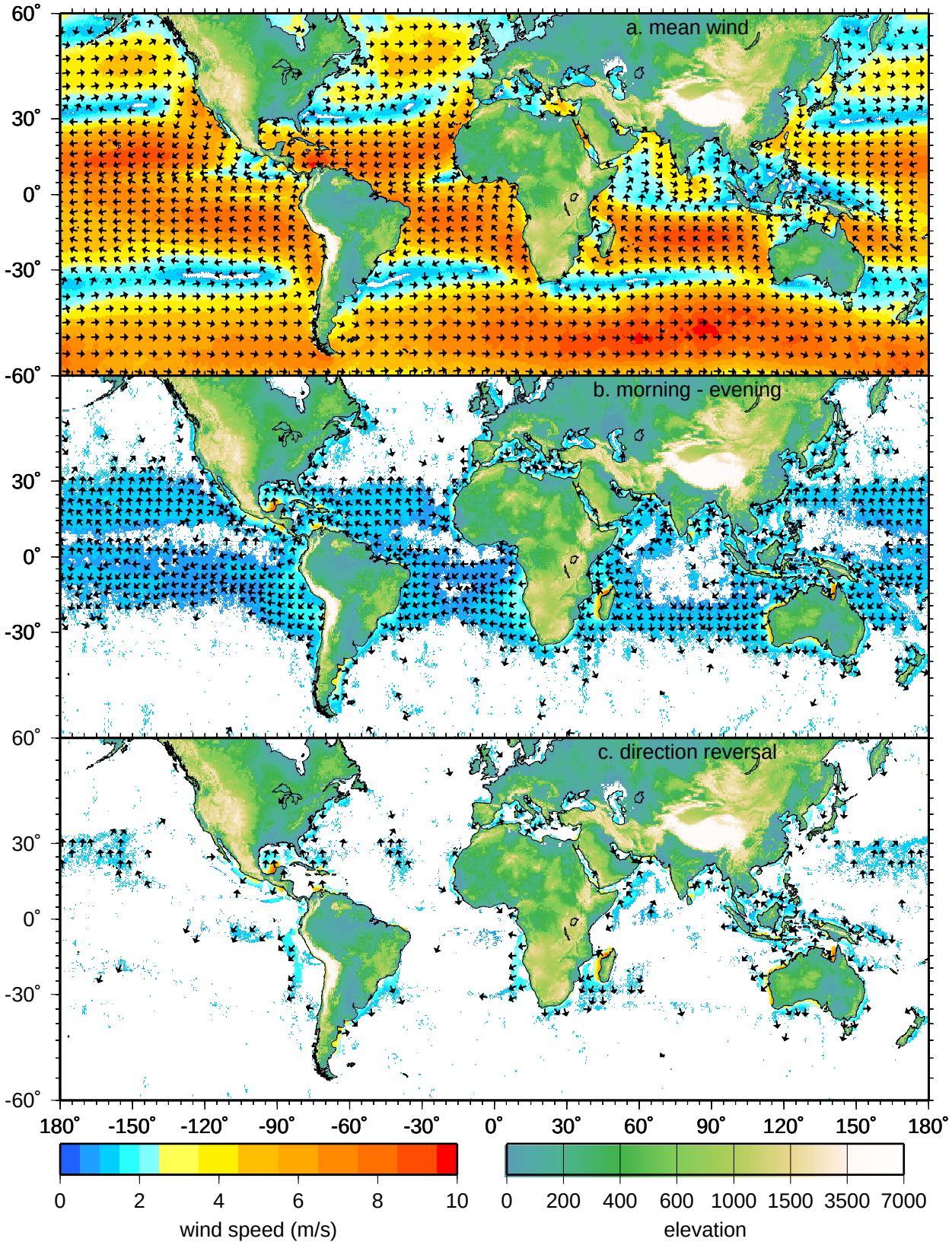

Figure 2. Amplitude (color) and direction (vectors) of winds. (a) Average of mean morning and evening winds. (b) Mean morning minus evening winds. (c) As (b), but regions where the flow does not reverse are excluded. Wind velocity differences that are not statistically significant are shown as white. Vectors are plotted at 4 degree intervals, except in (a), where the zonal separation between vectors is 6 degrees. Landmasses are shaded to show elevation above sea level, based on the ETOPO2 data base.

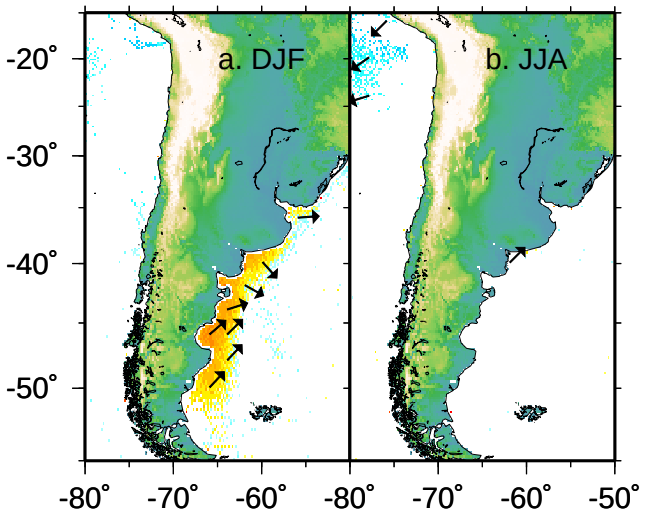

Figure 3. Seasonal cycle for mean evening minus morning winds off South America as in Figure 2c, but based on 0.2° by 0.2° boxes, with vectors shown every 2 degrees. (a) December, January, February. (b) June, July, August.